Zinc-dependent mechanical properties of *Staphylococcus aureus* biofilm-forming surface protein SasG

Cécile Formosa-Dague[a], Pietro Speziale[b], Timothy J. Foster[c], Joan A. Geoghegan[c,1], and Yves F. Dufrêne[a,d,1]

[a]Institute of Life Sciences, Université Catholique de Louvain, B-1348 Louvain-la-Neuve, Belgium; [b]Department of Molecular Medicine, Unit of Biochemistry, University of Pavia, 27100 Pavia, Italy; [c]Department of Microbiology, Trinity College Dublin, Dublin 2, Ireland; and [d]Walloon Excellence in Life Sciences and Biotechnology, B-1300 Wavre, Belgium

Edited by Scott J. Hultgren, Washington University School of Medicine, St. Louis, MO, and approved December 2, 2015 (received for review September 29, 2015)

Staphylococcus aureus **surface protein SasG promotes cell–cell adhesion during the accumulation phase of biofilm formation, but the molecular basis of this interaction remains poorly understood. Here, we unravel the mechanical properties of SasG on the surface of living bacteria, that is, in its native cellular environment. Nanoscale multiparametric imaging of living bacteria reveals that Zn^{2+} strongly increases cell wall rigidity and activates the adhesive function of SasG. Single-cell force measurements show that SasG mediates cell–cell adhesion via specific Zn^{2+}-dependent homophilic bonds between β-sheet–rich G5–E domains on neighboring cells. The force required to unfold individual domains is remarkably strong, up to ∼500 pN, thus explaining how SasG can withstand physiological shear forces. We also observe that SasG forms homophilic bonds with the structurally related accumulation-associated protein of *Staphylococcus epidermidis*, suggesting the possibility of multispecies biofilms during host colonization and infection. Collectively, our findings support a model in which zinc plays a dual role in activating cell–cell adhesion: adsorption of zinc ions to the bacterial cell surface increases cell wall cohesion and favors the projection of elongated SasG proteins away from the cell surface, thereby enabling zinc-dependent homophilic bonds between opposing cells. This work demonstrates an unexpected relationship between mechanics and adhesion in a staphylococcal surface protein, which may represent a general mechanism among bacterial pathogens for activating cell association.**

Staphylococcus aureus | biofilms | adhesion | SasG | atomic force microscopy

The bacterial pathogen *Staphylococcus aureus* causes a wide range of infections in humans, which are often associated with the ability of the bacteria to form biofilms on indwelling medical devices such as central venous catheters and prosthetic joints (1–4). Biofilm formation involves initial adhesion of the bacteria to surfaces, followed by cell–cell adhesion (aggregation) to form microcolonies and a mature biofilm, and finally dispersal by the detachment of cell aggregates from the biofilm (5). Currently, little is known about the molecular interactions driving biofilm formation by *S. aureus* due to the paucity of appropriate high-resolution probing techniques. Such knowledge may contribute to the development of novel compounds for therapy.

Adhesion and biofilm formation by *S. aureus* involve a variety of cell wall components. Whereas adhesion to host proteins is mediated by cell-wall–anchored (CWA) proteins (6, 7), intercellular adhesion was until recently thought to be promoted by the expression of the polysaccharide intercellular adhesin (PIA), also known as the poly-*N*-acetyl-glucosamine (PNAG) (8, 9). This positively charged polymer is able to bind the negatively charged bacterial surfaces. PIA, encoded by genes in the *ica* operon, represents the most well-understood biofilm-mediating pathway in staphylococci (10, 11). However, many strains do not produce PIA and rely on CWA proteins to promote intercellular adhesion in an *ica*-independent manner (6, 7).

A prototype of biofilm-forming CWA protein is SasG (12–15), which mediates cell–cell adhesion through its "B" multidomain region (5, 7). B repeat sequences contain "G5" domains (∼78 residues) in a tandem array, separated by 50-residue sequences known as the "E" regions (Fig. 1*A*) (14, 15). SasG forms β-sheet–rich protein fibrils that protrude from the cell surface, which can be visualized by electron microscopy (12). The proposed mechanism for SasG-mediated cell association is based on homophilic protein–protein interactions. SasG is covalently attached to the cell wall and undergoes limited cleavage within the B region to remove the N-terminal "A" region. The cleaved and exposed SasG B domains on neighboring cells interact with each other in a Zn^{2+}-dependent manner, leading to cell–cell adhesion (13). The G5–E domains of the related accumulation-associated protein (Aap) of *Staphylococcus epidermidis* are also responsible for the Zn^{2+}-dependent biofilm formation (15). However, recent work also suggests that Aap could bind a ligand protein, the small basic protein (Sbp), which accumulates on the cell surface and within the biofilm matrix (16). Therefore, whereas SasG and Aap are believed to mediate intercellular adhesion via zinc-dependent homophilic bonds between opposing proteins, it is unclear whether this is the only mechanism at play. Also, the mode of action of zinc is controversial. Whereas

Significance

Hospital-acquired infections often involve surface-associated microbial communities called biofilms that show increased resistance to antibiotics. A molecular understanding of the fundamental interactions driving adhesion and biofilm formation by microbial pathogens is a key step toward the development of novel antimicrobial therapies. Here we demonstrate that the SasG surface protein from *Staphylococcus aureus* displays remarkable zinc-dependent mechanical properties that are critical for its adhesive function during biofilm formation. We find that zinc activates SasG-mediated adhesion through a mechanism whereby adsorption of zinc ions to the bacterial cell surface increases cell wall cohesion and favors zinc-dependent homophilic bonds between SasG proteins protruding from opposing cell surfaces. The zinc-dependent adhesive function of SasG represents a promising target for the design of antibacterial compounds.

Author contributions: C.F.-D., P.S., T.J.F., J.A.G., and Y.F.D. designed research; C.F.-D. performed research; C.F.-D., P.S., T.J.F., J.A.G., and Y.F.D. analyzed data; and C.F.-D., P.S., T.J.F., J.A.G., and Y.F.D. wrote the paper.

The authors declare no conflict of interest.

This article is a PNAS Direct Submission.

[1]To whom correspondence may be addressed. Email: yves.dufrene@uclouvain.be or geoghegj@tcd.ie.

This article contains supporting information online at www.pnas.org/lookup/suppl/doi:10.1073/pnas.1519265113/-/DCSupplemental.

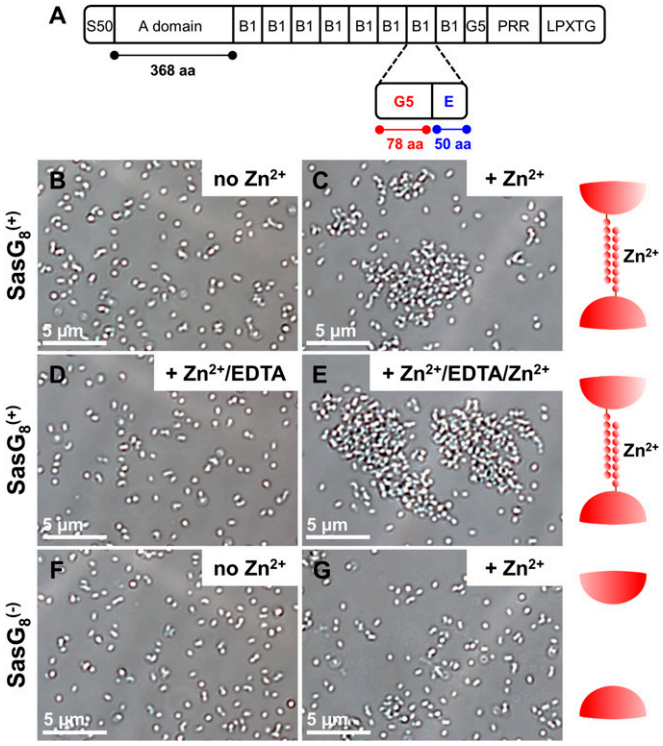

Fig. 1. Role of SasG in cell–cell adhesion. (*A*) Schematic representation of the SasG structure emphasizing the A domain, not engaged in cell–cell adhesion, and the B repeat sequence containing G5 domains (78 residues) in a tandem array, separated by the E regions (50 residues). (*B–E*) Optical microscopy images of *S. aureus* cells expressing full-length SasG [$SasG_8^{(+)}$ cells] after resuspension in TBS buffer (*B*) or in TBS buffer containing 1 mM of $ZnCl_2$ (*C*), after addition of 1 mM EDTA (*D*), and further addition of 1 mM $ZnCl_2$ (*E*). (*F* and *G*) Control experiment using *S. aureus* expressing no SasG [$SasG^{(-)}$ cells] in TBS buffer (*F*) or in TBS containing 1 mM of $ZnCl_2$ (*G*).

SasG dimerizes in vitro in a zinc-dependent manner, a direct link between homodimerization and biofilm formation has not yet been established. Rather, it has been suggested that zinc could mediate binding to anionic cell surface components like teichoic acids (14). Direct biophysical analysis of SasG proteins on the surface of living cells would help to clarify these important issues.

Recent advances in atomic force microscopy (AFM) techniques have enabled researchers to gain insight into the biophysical properties and molecular interactions of microbial cells (17, 18), including *S. aureus* (19–22). A variety of AFM-based force spectroscopy methods have been developed, in which the force acting on the AFM probe is measured with piconewton (10^{-12} N) sensitivity as the probe is pushed toward the sample, then retracted from it (17). In the past few years, a new force spectroscopy-based imaging mode, multiparametric imaging, has offered the possibility to image the surface structure of living cells, while mapping their mechanical and adhesive properties at unprecedented spatiotemporal resolution (23–28). Unlike in conventional imaging, the method involves recording arrays of force curves across the cell surface, at improved speed, positional accuracy, and force sensitivity (26). As the curves are recorded at high frequency, correlated images of the structure, adhesion, and mechanics of the cells can be obtained at the speed of conventional imaging. This technology has been used to image single filamentous bacteriophages extruding from living bacteria (25) and to map adhesive nanodomains on fungal pathogens (28). Furthermore, recent progress in single-cell force spectroscopy (SCFS) (18, 29, 30) has made it possible to understand the forces driving cell adhesion and biofilm formation. Here, a living cell is attached to the AFM probe, thereby enabling researchers to measure the interaction forces between the cell and a target surface (18). Applying these newly developed modalities to staphylococci is a challenging problem, which would provide novel insights into the molecular bases of biofilm formation and biofilm-associated infections.

Here, we combine multiparametric imaging and SCFS to investigate the mechanical strength of SasG on living bacterial cells, thus in its fully functional environment. We use a *S. aureus* strain carrying a plasmid expressing SasG with eight consecutive G5–E repeats [hereafter *S. aureus* $SasG_8^{(+)}$ cells]. We show that intercellular adhesion involves the Zn^{2+}-dependent–specific association of G5–E repeats on opposing cells and that the elongated structure and mechanical strength of SasG make it ideally suited for that purpose. In addition, our results show that Zn^{2+} plays a dual role that is more complex than anticipated before: adsorption of Zn^{2+} to cell wall components increases the cohesion of the cell surface, thereby favoring the projection of highly elongated SasG proteins beyond other surface components and making them fully functional for Zn^{2+}-dependent homophilic interactions.

Results

SasG Mediates Intercellular Adhesion. We first studied the involvement of SasG in cell–cell adhesion at the microscale (Fig. 1 *B–G*). Fig. 1*B* shows that $SasG_8^{(+)}$ cells suspended in buffer did not form aggregates. Upon addition of 1 mM Zn^{2+}, cell aggregates, 5–10 µm in size, were observed (Fig. 1*C*). Addition of 1 mM EDTA disrupted the cell aggregates (Fig. 1*D*), whereas further addition of Zn^{2+} restored them (Fig. 1*E*). Because aggregation was not observed in *S. aureus* cells expressing no SasG [$SasG_8^{(-)}$ cells; Fig. 1 *F* and *G*], we conclude that SasG promotes Zn^{2+}-dependent intercellular adhesion, in line with earlier reports (13, 14).

Zn^{2+} Strongly Alters the Structural, Mechanical, and Adhesive Properties of the Cell Surface. In view of the role of zinc in intercellular adhesion, we investigated the influence of this metal on the biophysical properties of the cell surface. To this end, living bacteria were probed at the nanoscale using the new multiparametric imaging technology. Fig. 2 *A–L* presents simultaneous AFM images of the topography, elasticity, and adhesion of two $SasG_8^{(+)}$ cells recorded with a silicon nitride tip. In the absence of zinc, the cells showed a rough surface morphology, a moderate cell wall stiffness, and very poor adhesive properties (Fig. 2 *A*, *E*, and *I*). To get further details on the cell surface structure, the cells were imaged in contact mode (Fig. S1 *A–C*). Both height and deflection images featured a fuzzy contrast, and the roughness on 500-nm × 500-nm height images was 2.5 ± 1 nm (mean ± SD from five different cells). As $SasG_8^{(+)}$ and $SasG_8^{(-)}$ cells showed similar morphology (Fig. 2*M* and Fig. S1 *G–I*) and roughness (2.7 ± 0.5 nm), the observed structural features are not associated with SasG.

To obtain quantitative information on cell wall mechanical properties, we determined the Young modulus of the bacteria (Fig. 2*E*). This parameter reflects the resistance of the cell wall to compression (the higher the Young modulus, the stiffer the cell wall), and is obtained by converting force curves into force vs. indentation curves, and analyzing these curves with theoretical models like the Hertz model (Fig. S2 *A* and *B*; for detailed information, see ref. 31). Fig. S2 *A* and *B* shows that the bacterial Young modulus was 495 ± 272 kPa (mean ± SD on a total of $n = 3{,}072$ curves from three different cells). This moderate cell wall stiffness, in line with earlier measurements on *S. aureus* (20), reflects the elasticity of peptidoglycan together with other cell wall components. Adhesion images were also recorded in parallel to probe the adhesive character of the cell surface (Fig. 2*I*). The maximum adhesion force was assessed in every force curve and the value displayed as a colored pixel (the brighter the pixel, the stronger the adhesion). The lack of adhesion contrast that we observed means that the cells poorly adhered to AFM tips, thus that, in the absence of zinc, SasG does not convey adhesive properties to the cell surface.

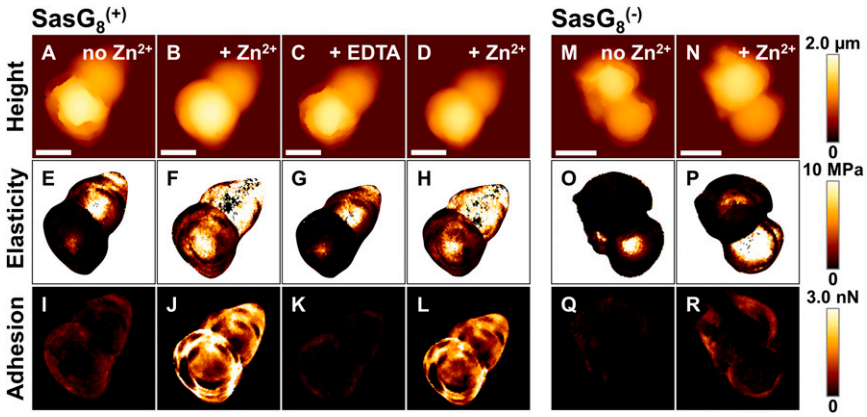

Fig. 2. Nanoscale multiparametric imaging unravels the structural and biophysical properties of *S. aureus*. (*A*) Height image of two dividing *S. aureus* cells expressing SasG [$SasG_8^{(+)}$] in TBS buffer and simultaneous (*E*) Young modulus and (*I*) adhesion image. Data were obtained in the same conditions following addition of 1 mM $ZnCl_2$ (*B*, *F*, and *J*), of 1 mM $ZnCl_2$ then 1 mM of EDTA (*C*, *G*, and *K*), and following further addition of 1 mM of $ZnCl_2$ (*D*, *H*, and *L*). Control experiment using *S. aureus* cells expressing no SasG [$SasG_8^{(-)}$] in TBS buffer (*M*, *O*, and *Q*) or in TBS containing 1 mM $ZnCl_2$ (*N*, *P*, and *R*). (Scale bars: 1 µm.) Similar results were obtained for five $SasG_8^{(+)}$ cells and five $SasG_8^{(-)}$ cells from different cultures.

Remarkably, addition of zinc strongly altered the structural, mechanical, and adhesive properties of the cell surface (Fig. 2 *B*, *F*, and *J*). The surface morphology, also shown in Fig. S1 *D–F*, was much smoother and better defined, with a roughness of only 0.4 ± 0.1 nm, an effect that we attribute to a change in the organization and cohesion of the cell wall components. Supporting this view, the cell surface was stiffer, with a Young modulus of 1,092 ± 377 kPa (Fig. 2*F* and Fig. S2 *A* and *C*). Note that the Hertz model used to assess the Young modulus is valid for elastic surfaces and does not take into account tip-sample adhesion. Although the adhesion force (~400 pN) was much smaller than the maximum applied force (5 nN), absolute values of Young modulus should be considered with caution. In the future, it would be interesting to test the JKR (Johnson, Kendall, and Roberts) model, which applies to strongly adhesive samples. Nevertheless, the major change in the slopes of the force vs. indentation curves (Fig. S2*A*) clearly demonstrates an increase in cell wall stiffness. Cells lacking SasG proteins [$SasG_8^{(-)}$] in the presence of Zn^{2+} exhibited rougher surfaces (roughness of 1.4 ± 0.5 nm, Fig. S1 *G–I*) and a Young modulus of either 566 ± 149 kPa or 1,081 ± 142 kPa (Fig. 2*P* and Fig. S2 *D* and *F*). So, for some of the probed areas, the cell surface showed a stiffness similar to that of $SasG_8^{(+)}$ cells in the presence of Zn^{2+}, whereas in other areas it was softer. This finding suggests that SasG contributes only moderately to the cell surface stiffness. Presumably, Zn^{2+} ions bind, crosslink, and collapse negatively charged cell wall components, like the polyphosphate groups of teichoic acids and the carboxyl units of peptidoglycan, thereby increasing the rigidity of the cell surface. We also found that Zn^{2+} dramatically increased the adhesive properties of $SasG_8^{(+)}$ cells (Fig. 2*J*). As $SasG_8^{(-)}$ cells did not show such an effect (Fig. 2*R*), we conclude that the zinc-dependent adhesive properties of the cells are due to SasG. $SasG_8^{(+)}$ cells showed homogeneous adhesive contrast, indicating that the protein was uniformly exposed on the cell surface. These data show that SasG strongly binds to the silicon nitride tip. As the tip surface bears negative charges, we expect that Zn^{2+} ions will promote SasG–tip interactions via electrostatic bridges. The changes in structural and biophysical properties were reversed in the presence of 1 mM EDTA (Fig. 2 *C*, *G*, and *K*) and restored upon further addition of Zn^{2+} (Fig. 2 *D*, *H*, and *L*), thus indicating that the cell surface remodeling was highly dynamic and reversible.

Next, we asked whether these cell surface changes could also be induced by other divalent ions. We found that addition of Ca^{2+} (Fig. S3) did not alter the structural, mechanical, and adhesive properties of the cell surface (surface roughness of 2.7 ± 0.9 nm; Young modulus of 507 ± 249 kPa), leading us to conclude that the staphylococcal cell surface dynamics demonstrated here depends specifically on Zn^{2+}. The zinc-dependent elasticity and adhesion were correlated with the adhesion phenotype observed on the microscale (Fig. 1), suggesting strongly that these nanoscale cell surface properties are critical to intercellular adhesion.

In summary, multiparametric imaging has revealed an unanticipated and complex connection between the structural and physical dynamics of the *S. aureus* cell wall, which is tightly controlled by Zn^{2+} ions. We believe that the zinc-induced stiffening and smoothening of the cell surface will favor the projection of highly elongated SasG fibrils beyond other surface components, making them fully available for interaction. To further support the validity of this model, SasG proteins were specifically detected on the bacterial cell surface using single-molecule imaging (17). Adhesion force maps were recorded across the cell surface using AFM tips modified with a monoclonal antibody directed against SasG G5–E repeats (Fig. S4). In the absence of zinc, the surface of $SasG_8^{(+)}$ cells showed weak adhesion, indicating that SasG was poorly detected (Fig. S4*A*). By contrast, addition of zinc dramatically increased the adhesion forces (Fig. S4*B*), with many of the force profiles showing multiple force peaks with long ruptures (Fig. S4*C*). As these features were not observed with $SasG_8^{(-)}$ cells (Fig. S4 *D–F*), they are attributed to the force-induced unfolding of individual G5–E repeats (see also Fig. 4 below for details). So, single-molecule imaging and multiparametric imaging demonstrate that zinc induces the massive exposure of SasG proteins on the cell surface.

Force Spectroscopy Uncovers the Mechanical Strength of SasG Bonds in Living Cells. Is SasG engaged in homophilic bonds or in receptor–ligand bonds? How strong are these bonds and how do they respond to mechanical force? To answer these pertinent questions, force–distance curves were recorded between two individual *S. aureus* cells using SCFS. Fig. 3 shows the force data—i.e., maximum adhesion force and rupture length histograms—obtained after a contact time of 100 ms for three representative pairs of $SasG_8^{(+)}$ cells. The maximum adhesion force corresponds to the largest adhesion event in each force curve, whereas the rupture length is the distance of the last adhesion event, thus where the two cells separate. In the absence of Zn^{2+}, cells hardly adhered to each other (adhesion frequency ranging from 5 to 31%). By contrast, addition of Zn^{2+} dramatically enhanced cell–cell adhesion, the adhesion frequency increasing up to 80–100%. Force curves generally showed multiple

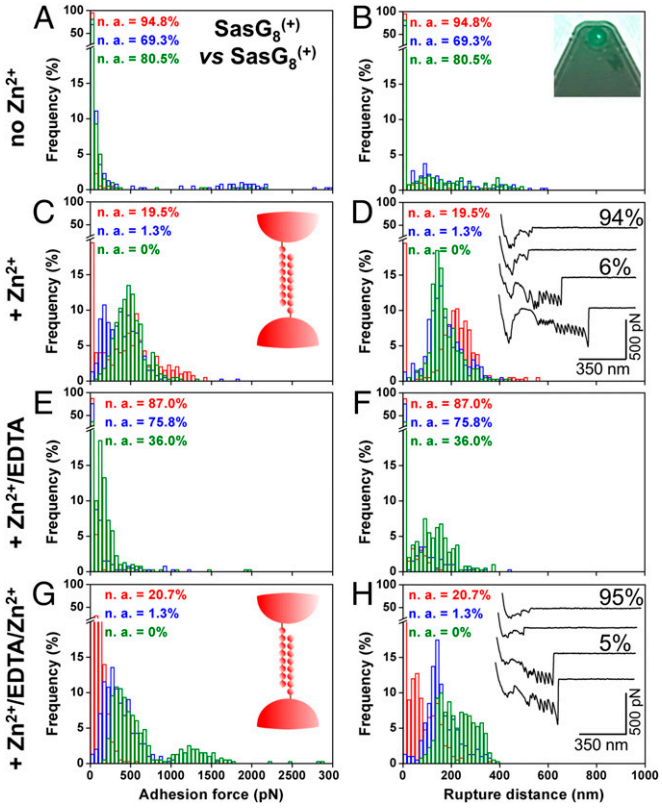

Fig. 3. Single-cell force spectroscopy of SasG bonds. (*A*) Adhesion force and (*B*) rupture distance histograms obtained in TBS buffer for three pairs (see three different colors) of *S. aureus* cells expressing full-length SasG [$SasG_8^{(+)}$]. "n.a." values are the percentages of nonadhesive events. *Inset* in *B* is a fluorescence image of a single bacterium attached to the colloidal probe. (*C*–*H*) Force data obtained in the same conditions following addition of 1 mM of $ZnCl_2$ (*C* and *D*), of 1 mM of $ZnCl_2$, then 1 mM of EDTA (*E* and *F*), and following further addition of 1 mM of $ZnCl_2$ (*G* and *H*). *Insets* in *D* and *H* show representative force signatures and their occurrence (n = 1,200 curves in each condition). All curves were obtained using a contact time of 0.1 s, an applied force of 250 pN, and an approach and retraction speed of 1.0 μm/s.

peaks with a maximum adhesion force of 414 ± 222 pN magnitude and a rupture length of 182 ± 76 nm (mean ± SD on a total of n = 2,000 adhesive curves from five cells). Only small variations were observed from one cell pair to another, indicating that cell populations were homogeneous and showed reproducible properties from one culture to another. The SasG-dependent cell–cell adhesion forces measured here are smaller than those reported for another *S. aureus* CWA protein, fibronectin-binding protein A (FnBPA, up to 2,000 pN) (32). However, FnBPA-dependent cell–cell adhesion was estimated to involve about 10 cumulative homophilic bonds, whereas here, the observation of reproducible and well-defined unfolding signatures leads us to believe that they primarily involves single (few) protein pairs. Cell–cell adhesion was strongly inhibited upon addition of EDTA (Fig. 3 *E* and *F*), the mean adhesion frequency and maximum adhesion force decreasing to 34% and 121 ± 56 pN (mean ± SD on a total of n = 2,000 adhesive curves from five cells), and restored upon further addition of Zn^{2+} (Fig. 3 *G* and *H*; adhesion frequency: 93%; adhesion force: 373 ± 167 pN). Multipeak force profiles were no longer seen in EDTA but restored when Zn^{2+} was added again. When Ca^{2+} was used instead of Zn^{2+}, the cells showed hardly any adhesive interactions (Fig. S3), demonstrating the specificity of the zinc-dependent cell–cell adhesion. These results show that the adhesive and mechanical properties of SasG are highly dynamic and zinc dependent, in agreement with our multiparametric data.

A substantial fraction (~6%) of adhesive curves recorded in the presence of zinc showed multiple force peaks that were equally spaced (Fig. 4). These sawtooth patterns are reminiscent of those observed when stretching modular proteins such as titin and fibronectin (33); they originate from the force-induced unfolding of protein secondary structures (α-helices, β-sheets). Some sawtooth profiles (Fig. 4) featured low force peaks (330 ± 38 pN, n = 51), followed by high force peaks (512 ± 40 pN, n = 58). The peaks were well fitted by the worm-like chain (WLC) model (33), supporting further the notion they reflect the unfolding of multidomain proteins. From the fits (blue and red lines in Fig. 4*A*), we extracted the protein contour length, L_c, i.e., the length of the fully extended molecule, and found that the gains in L_c were constant: $\Delta L_c = 14 \pm 2$ ($n = 51$) and $\Delta L_c = 21 \pm 1$ ($n = 58$) for the low and high force peaks, respectively (Fig. 4*C*). Assuming that each residue contributes 0.38 nm to the contour length of a fully extended polypeptide chain and that the folded lengths of the E and G5 domains are 4.5 and 7.0 nm (34), our measured ~14- and ~21 nm-increments match the expected 50 and 78 residues of single E and G5 domains. This result, together with control experiments (Fig. S5), leads us to conclude that low and high force peaks represent the sequential unfolding of E and G5 domains.

The unfolding forces of SasG measured on live cells are in the range of those determined in vitro for purified SasG using similar pulling speed (34), but larger than unfolding forces reported for strong β-fold domains (150–300 pN), such as Ig and fibronectin domains (33), thus indicating that SasG is a mechanically strong protein. The G5–E domains are composed of flat, single-layer β-sheets lacking a compact hydrophobic core, explaining how SasG forms thin filaments on the cell surface (14). Molecular dynamics (MD) simulations (34) revealed that the mechanical strength of SasG domains originates from tandemly arrayed mechanical clamps involving long stretches of hydrogen bonds and associated side-chain packing interactions along the β-strands. Whereas E and G5 repeats are structurally similar, the E segment has shorter N-terminal clamps and therefore has been shown to be significantly less stable than G5 (14). SasG extension has been shown to involve obligate folding cooperativity of the E domains that couple nonadjacent G5 domains, forming interfaces that are more stable than

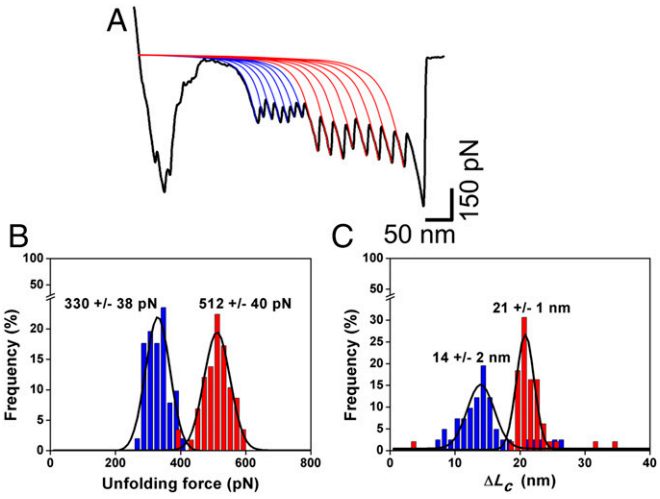

Fig. 4. Mechanical strength of SasG domains. (*A*) Representative force curve displaying sawtooth profiles with up to eight low force peaks followed by eight high force peaks, that were well fitted with the extensible worm-like-chain (WLC) model using a persistence length l_p of 0.4 nm (blue and red lines). (*B*) Unfolding force and (*C*) contour length gain (ΔLc) histograms documenting the sequential unfolding of E domains (blue; n = 51), followed by the more stable G5 domains (red; n = 58).

MICROBIOLOGY

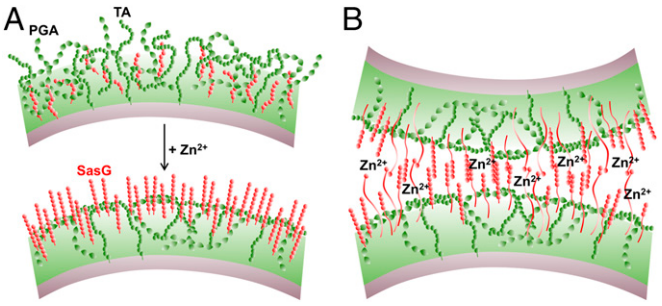

Fig. 5. Proposed model for the zinc-dependent activation of intercellular adhesion. (*A*) Zn^{2+} alters the cell wall organization thereby making SasG fully functional. In the absence of Zn^{2+}, cell wall components including negatively charged teichoic acids (TAs) and poly-γ-glutamic acid (PGA), are freely distributed and protrude from the cell surface, therefore masking SasG proteins. Addition of Zn^{2+} dramatically alters the cell wall organization by interaction with negatively charged TA and PGA. Zn^{2+} binding increases the cell surface stiffness and decreases the cell surface roughness, allowing SasG proteins to be fully available for interaction. (*B*) Zn^{2+} promotes homophilic bonds between protruding SasG repeats on opposing cells, thereby leading to intercellular adhesion. For the sake of clarity the A domain is not shown.

the domains themselves (34). Unlike the in vitro force profiles (34), unfolding signatures on live cells often showed low (E domains) and high (G domains) force peaks that were randomly distributed (Fig. 3*D*). This complex mechanical response may be associated with the unfolding of SasG domains engaged in homophilic bonds.

We believe that the multimodular structure and remarkable mechanical strength of SasG are related to the protein's function. During biofilm development, the elongated, rod-like shape of the adhesin will play a key role in bridging cells together. Owing to its mechanical strength, SasG will resist physiological shear forces and maintain cell–cell contacts. Under high mechanical force, the sequential unfolding of SasG B repeats may expose extended conformations in which previously masked adhesive residues may become available for interaction. A pertinent question is whether there is a functional advantage for SasG to alternate E and G5 domains. Gruszka et al. (34) suggested that the less stable E domains may behave as force buffers capable of relieving mechanical stress without complete unfolding of the SasG molecule. Thus, the protein may switch between a flexible state under force, and a stiff state with all domains folded when no force is applied.

Another interesting observation is that unfolding profiles were seen at rather long distances, starting at 151 ± 50 nm (n = 164 curves; five cells) and were generally preceded by poorly defined adhesive events. This observation indicates that B repeat unfolding was preceded by the deformation of another large region of the protein, i.e., the A domain. Unfolding of a single A domain made of 368 amino acids should yield protein extensions of ∼132 nm. Considering that the straightening of the folded G5–E chain will also contribute to protein extension, our ∼150-nm length is consistent with the unfolding of A domains. Geoghegan et al. (13) showed that full-length SasG proteins on *S. aureus* are processed within the B domains, yielding cleaved proteins of various lengths at the cell surface. Our data suggest that at least a fraction of SasG proteins retain their full-length structure on the cell surface.

It is tempting to speculate on the molecular basis for the measured SasG cell–cell adhesion forces. Early work has revealed that tandem G5 domains associate in a zinc-dependent modular fashion, suggesting a zinc zipper model for G5-domain–based intercellular adhesion in staphylococcal biofilms (35). In such a model, we expect that multiple interactions between two proteins should disrupt one by one along the applied force, giving rise to constant force plateau signatures (36). As this result was not observed here, our data argue against a zipper model. More recently, X-ray crystallography analysis (15) has suggested a twisted rope-like structure between bacterial cells, in which the antiparallel monomers wrap around one another. Hence, the β-sheet unfoldings we observed when separating two cells might be associated with the rupture of rope-like bonds.

Intercellular Adhesion Involves Homophilic Bonds Between G5–E Domains. To further understand the mechanisms of SasG-mediated adhesion, we analyzed the forces between *S. aureus* $SasG_8^{(-)}$ cells, which express no SasG proteins on their surface (Fig. S5). Most curves recorded in the presence of Zn^{2+} showed no adhesion, demonstrating that the large adhesion forces on $SasG_8^{(+)}$ cells are mediated by SasG. Analysis of the forces between $SasG_8^{(+)}$ and $SasG_8^{(-)}$ cells (Fig. S5 *C* and *D*) led to the same observation, implying that the bonds between $SasG_8^{(+)}$ cells involve SasG molecules on both cells. So, our data provide direct evidence that SasG mediates cell–cell adhesion through homophilic bonds rather than receptor–ligand binding. Hence, our work is not in favor of the model in which SasG would bind ligands on opposing cells, as was recently proposed for the interaction between Aap and the small protein Sbp, which accumulates on cells and within the biofilm matrix (16).

We also probed *S. aureus* $SasG_1^{(+)}$ cells, which express SasG with single G5–E repeats (Fig. S5 *E* and *F*). Many curves were poorly adhesive, indicating that proteins with only one B repeat are not capable of mediating adhesion. Supporting further this view, multiparametric adhesion maps recorded with a silicon nitride tip showed very little adhesion even in the presence of zinc (Fig. S5 *G* and *H*). These data show that the multidomain, rod-like structure of SasG is essential for its function.

SasG Forms Homophilic Bonds with the Structurally Related Aap Protein. The Aap protein from *S. epidermidis* (15, 35) has structural and functional properties similar to those of SasG. We therefore hypothesized that these two proteins might interact together by forming zinc-dependent homophilic bonds. Fig. S6 shows force data obtained between *S. aureus* $SasG_8^{(+)}$ cells and *S. epidermidis* $Aap^{(+)}$ cells expressing, on average, eight B repeats. In the presence of Zn^{2+}, strong adhesion was observed, with an adhesion frequency of 50–100%. Control experiment with $SasG_8^{(-)}$ cells (Fig. S6 *E–H*) showed that this interaction is specific to SasG. Force curves generally showed multiple peaks and a maximum adhesion force of 161 ± 79 pN magnitude and a rupture length of 168 ± 129 nm (mean ± SD, n = 2,000 adhesive curves from five cells), thus with a lower force than for the $SasG_8^{(+)}$–$SasG_8^{(+)}$ interaction. Hence, owing to their strong structural similarities, SasG and Aap can form homophilic bonds, thereby providing an elegant means to promote interspecies interactions in biofilms. This hitherto undescribed ability of *S. aureus* and *S. epidermidis* surface proteins to form homophilic bonds might be important during the formation of multispecies biofilms during infection.

Discussion

The role of cell surface mechanics in bacterial adhesion is an important yet poorly understood issue. By means of newly developed AFM techniques, we have shown that the zinc-dependent nanomechanical properties of SasG play a key role in defining its adhesive function, providing a molecular foundation for its ability to mediate cell association during biofilm formation. Unlike in vitro biomolecular assays, our live-cell experiments enabled us uniquely to analyze functional SasG proteins directly on the surface of live cells, thus in a biologically relevant conformation. Recombinant CWA protein domains purified from the cytoplasm of *Escherichia coli* may fold differently and impurities may be present that could influence functional activity in vitro. Therefore, it is very challenging to develop live-cell nanoscopy methods to study proteins that have been secreted through the cell membrane, anchored to the cell wall peptidoglycan and displayed in the *S. aureus* cell surface environment.

The strength of SasG-mediated interactions was quantified, showing that it represents a major driving force for cell–cell adhesion. The SasG G5–E domains are engaged in specific

Zn^{2+}-dependent homophilic bonds, rather than in receptor–ligand bonds. Loading these bonds with mechanical force leads to the sequential unfolding of mechanically strong E and G5 domains. Intercellular forces are not observed with bacteria expressing SasG with single G5–E repeats, confirming that the elongated multidomain structure of SasG is important for cell–cell association. The remarkable strength of the protein is consistent with tandemly arrayed clamp motifs within the folded domains, explaining how bacteria in the biofilm are capable of withstanding physiological shear forces. We expect that under high mechanical stress, SasG domains will unfold and may expose extended conformations with enhanced adhesive properties.

We discovered a previously unidentified role for zinc, that is, controlling the relationship between bacterial cell wall mechanics and the adhesive function of SasG. Collectively, our results support a model (Fig. 5) whereby zinc activates intercellular adhesion not only by promoting SasG homophilic bonds, but also by inducing the collapse of cell surface constituents, triggering the projection of highly elongated SasG structures beyond other surface components, and in turn, enabling homophilic binding between opposing cells. Finally, owing to strong structural similarities, SasG and Aap are capable of forming zinc-dependent homophilic bonds, thus promoting interspecies interactions in mixed biofilms.

In conclusion, our study demonstrates an unexpected relationship between nanomechanics and adhesion in a staphylococcal surface protein and highlights the complex influence of zinc ions in activating the protein function. Zinc-dependent cell surface dynamics may represent a general mechanism for activating adhesion in biofilm-forming species. Controlling this phenomenon may provide a means for developing antibiofilm strategies.

Methods

The following *S. aureus* strains were used in this study: *S. aureus* strain SH1000 containing the plasmid pALC2073sasG$^+$ or an empty vector (13) *S. epidermidis* strain 1457 (wild-type strain) or its Δ*aap* mutant strain (37). Bacteria were grown in tryptic soy broth (TSB) supplemented with chloramphenicol (10 μg/mL) for *S. aureus*, or with tetracycline (5 μg/mL) for *S. epidermidis* Δ*aap* strain, at 37 °C, under agitation (180 rpm) until stationary phase was reached. Before AFM experiments, cells were harvested by centrifugation (1,000 × *g*, 3 min) and washed two times in Tris buffer saline (TBS, Tris 50 mM, NaCl 150 mM, pH = 7.4). Aggregation assays and AFM methods are described in *SI Methods*.

ACKNOWLEDGMENTS. We thank Sylvie Derclaye and David Alsteens for helping with the single-molecule imaging experiments. Work at the Université Catholique de Louvain was supported by the National Fund for Scientific Research (FNRS), the FNRS-Walloon Excellence in Life Sciences and Biotechnology (WELBIO) under Grant WELBIO-CR-2015A-05; the Federal Office for Scientific, Technical, and Cultural Affairs (Interuniversity Poles of Attraction Programme); and the Research Department of the Communauté Française de Belgique (Concerted Research Action). C.F.-D. holds a "MOVE-IN Louvain" Incoming Post-Doctoral Fellowship, cofounded by the Marie Curie Actions of the European Commission. Y.F.D. is a Research Director at the FNRS.

1. Costerton JW, Stewart PS, Greenberg EP (1999) Bacterial biofilms: A common cause of persistent infections. *Science* 284(5418):1318–1322.
2. López D, Vlamakis H, Kolter R (2010) Biofilms. *Cold Spring Harb Perspect Biol* 2(7): a000398.
3. Lister JL, Horswill AR (2014) *Staphylococcus aureus* biofilms: Recent developments in biofilm dispersal. *Front Cell Infect Microbiol* 4:178.
4. Hogan S, Stevens NT, Humphreys H, O'Gara JP, O'Neill E (2015) Current and future approaches to the prevention and treatment of staphylococcal medical device-related infections. *Curr Pharm Des* 21(1):100–113.
5. Hobley L, Harkins C, MacPhee CE, Stanley-Wall NR (2015) Giving structure to the biofilm matrix: An overview of individual strategies and emerging common themes. *FEMS Microbiol Rev* 39(5):649–669.
6. Speziale P, Pietrocola G, Foster TJ, Geoghegan JA (2014) Protein-based biofilm matrices in Staphylococci. *Front Cell Infect Microbiol* 4:171.
7. Foster TJ, Geoghegan JA, Ganesh VK, Höök M (2014) Adhesion, invasion and evasion: The many functions of the surface proteins of *Staphylococcus aureus*. *Nat Rev Microbiol* 12(1):49–62.
8. Otto M (2008) Staphylococcal biofilms. *Curr Top Microbiol Immunol* 322:207–228.
9. Mack D, et al. (1996) The intercellular adhesin involved in biofilm accumulation of *Staphylococcus epidermidis* is a linear beta-1,6-linked glucosaminoglycan: Purification and structural analysis. *J Bacteriol* 178(1):175–183.
10. O'Gara JP (2007) ica and beyond: Biofilm mechanisms and regulation in *Staphylococcus epidermidis* and *Staphylococcus aureus*. *FEMS Microbiol Lett* 270(2):179–188.
11. Laverty G, Gorman SP, Gilmore BF (2013) Biomolecular mechanisms of staphylococcal biofilm formation. *Future Microbiol* 8(4):509–524.
12. Corrigan RM, Rigby D, Handley P, Foster TJ (2007) The role of *Staphylococcus aureus* surface protein SasG in adherence and biofilm formation. *Microbiology* 153(Pt 8): 2435–2446.
13. Geoghegan JA, et al. (2010) Role of surface protein SasG in biofilm formation by *Staphylococcus aureus*. *J Bacteriol* 192(21):5663–5673.
14. Gruszka DT, et al. (2012) Staphylococcal biofilm-forming protein has a contiguous rod-like structure. *Proc Natl Acad Sci USA* 109(17):E1011–E1018.
15. Conrady DG, Wilson JJ, Herr AB (2013) Structural basis for Zn2+-dependent intercellular adhesion in staphylococcal biofilms. *Proc Natl Acad Sci USA* 110(3): E202–E211.
16. Decker R, et al. (2015) An 18 kDa scaffold protein is critical for *Staphylococcus epidermidis* biofilm formation. *PLoS Pathog* 11(3):e1004735.
17. Dufrêne YF (2014) Atomic force microscopy in microbiology: New structural and functional insights into the microbial cell surface. *MBio* 5(4):e01363–14.
18. Dufrêne YF (2015) Sticky microbes: Forces in microbial cell adhesion. *Trends Microbiol* 23(6):376–382.
19. Xu C-P, et al. (2008) *Staphylococcus aureus*-fibronectin interactions with and without fibronectin-binding proteins and their role in adhesion and desorption. *Appl Environ Microbiol* 74(24):7522–7528.
20. Francius G, Domenech O, Mingeot-Leclercq MP, Dufrêne YF (2008) Direct observation of *Staphylococcus aureus* cell wall digestion by lysostaphin. *J Bacteriol* 190(24): 7904–7909.
21. Lower SK, et al. (2010) A tactile response in *Staphylococcus aureus*. *Biophys J* 99(9): 2803–2811.
22. Casillas-Ituarte NN, Lower BH, Lamlertthon S, Fowler VG, Jr, Lower SK (2012) Dissociation rate constants of human fibronectin binding to fibronectin-binding proteins on living *Staphylococcus aureus* isolated from clinical patients. *J Biol Chem* 287(9): 6693–6701.
23. Heu C, Berquand A, Elie-Caille C, Nicod L (2012) Glyphosate-induced stiffening of HaCaT keratinocytes, a Peak Force Tapping study on living cells. *J Struct Biol* 178(1):1–7.
24. Alsteens D, et al. (2012) High-resolution imaging of chemical and biological sites on living cells using peak force tapping atomic force microscopy. *Langmuir* 28(49): 16738–16744.
25. Alsteens D, Trabelsi H, Soumillion P, Dufrêne YF (2013) Multiparametric atomic force microscopy imaging of single bacteriophages extruding from living bacteria. *Nat Commun* 4:2926.
26. Dufrêne YF, Martínez-Martín D, Medalsy I, Alsteens D, Müller DJ (2013) Multiparametric imaging of biological systems by force-distance curve-based AFM. *Nat Methods* 10(9):847–854.
27. Chopinet L, Formosa C, Rols MP, Duval RE, Dague E (2013) Imaging living cells surface and quantifying its properties at high resolution using AFM in QI™ mode. *Micron* 48: 26–33.
28. Formosa C, et al. (2015) Multiparametric imaging of adhesive nanodomains at the surface of *Candida albicans* by atomic force microscopy. *Nanomedicine (Lond)* 11(1): 57–65.
29. Helenius J, Heisenberg C-P, Gaub HE, Muller DJ (2008) Single-cell force spectroscopy. *J Cell Sci* 121(11):1785–1791.
30. Beaussart A, et al. (2013) Single-cell force spectroscopy of probiotic bacteria. *Biophys J* 104(9):1886–1892.
31. Touhami A, Nysten B, Dufrêne YF (2003) Nanoscale mapping of the elasticity of microbial cells by atomic force microscopy. *Langmuir* 19(11):4539–4543.
32. Herman-Bausier P, El-Kirat-Chatel S, Foster TJ, Geoghegan JA, Dufrêne YF (2015) *Staphylococcus aureus* fibronectin-binding protein A mediates cell-cell adhesion through low-affinity homophilic bonds. *MBio* 6(3):e00413–e00415.
33. Rief M, Gautel M, Oesterhelt F, Fernandez JM, Gaub HE (1997) Reversible unfolding of individual titin immunoglobulin domains by AFM. *Science* 276(5315):1109–1112.
34. Gruszka DT, et al. (2015) Cooperative folding of intrinsically disordered domains drives assembly of a strong elongated protein. *Nat Commun* 6:7271.
35. Conrady DG, et al. (2008) A zinc-dependent adhesion module is responsible for intercellular adhesion in staphylococcal biofilms. *Proc Natl Acad Sci USA* 105(49): 19456–19461.
36. Kellermayer MSZ, et al. (2005) Reversible mechanical unzipping of amyloid beta-fibrils. *J Biol Chem* 280(9):8464–8470.
37. Schaeffer CR, et al. (2015) Accumulation-associated protein enhances *Staphylococcus epidermidis* biofilm formation under dynamic conditions and is required for infection in a rat catheter model. *Infect Immun* 83(1):214–226.
38. Roche FM, Meehan M, Foster TJ (2003) The *Staphylococcus aureus* surface protein SasG and its homologues promote bacterial adherence to human desquamated nasal epithelial cells. *Microbiology* 149(Pt 10):2759–2767.
39. Köhler G, Milstein C (1975) Continuous cultures of fused cells secreting antibody of predefined specificity. *Nature* 256(5517):495–497.
40. Ebner A, et al. (2007) A new, simple method for linking of antibodies to atomic force microscopy tips. *Bioconjug Chem* 18(4):1176–1184.